Ultrasonic modulation of diffuse light in turbid media

Lihong V. Wang, Xuemei Zhao

Lihong V. Wang, Xuemei Zhao, "Ultrasonic modulation of diffuse light in turbid media," Proc. SPIE 2979, Optical Tomography and Spectroscopy of Tissue: Theory, Instrumentation, Model, and Human Studies II, (18 August 1997); doi: 10.1117/12.280273

SPIE.

Event: BiOS '97, Part of Photonics West, 1997, San Jose, CA, United States

Ultrasonic Modulation of Diffuse Light in Turbid Media

Lihong Wang* and Xuemei Zhao
Bioengineering Program
Texas A&M University
College Station, Texas 77843-3120

Abstract

Continuous-wave ultrasonic modulation of laser light has been used to image objects buried in tissue-simulating turbid media.[1,2] The ultrasonic wave focused into the turbid media modulated the laser light passing through the ultrasonic field. The modulated laser light collected by a photomultiplier tube reflected primarily the local mechanical and optical properties in the focal zone. Modulated signal was estimated using diffusion theory. The dependence of the ultrasound-modulated optical signal on the off-axis distance of the detector from the optic axis was studied. The mechanisms of ultrasonic modulation of light were discussed.

Key Words

Ultrasonic modulation, acousto-optics, optical imaging, optical tomography, turbid media.

Introduction

Nonionizing optical tomography of biological tissues including breast tissues has been an active research field as indicated by this volume and others.[3] The contrast mechanism of optical imaging is based on the difference in optical properties between diseased and surrounding normal biological tissues. Several optical imaging techniques being investigated include time-gated or time-resolved optical imaging, frequency-domain optical imaging, and optical coherence tomography. The time-resolved and frequency-domain techniques are mathematically linked by Fourier transform and have achieved comparable results, namely, several millimeter resolution for approximately five-centimeter thick tissues or tissue phantoms. Optical coherence tomography has achieved <10 μm resolution in both axial and lateral dimensions but is limited to a penetration depth of a couple of millimeters into biological tissues.

Because biological tissues are optically turbid media, light is quickly diffused inside tissues as a result of strong scattering. Light transmitted through tissues is classified into three categories:

* Corresponding author.
Tel: (409) 847-9040 Email: LWang@tamu.edu
Fax: (409) 847-9005 URL: http://biomed.tamu.edu/~lw

SPIE Vol. 2979 • 0277-786X/97/$10.00

ballistic light, quasi-ballistic light, and diffuse light. Ballistic light experiences no scattering by tissue and travels straight through the tissue and hence carries direct imaging information. Quasi-ballistic light experiences minimal forward-directed scattering and carries some imaging information. Diffuse light follows tortuous paths and carries little direct imaging information and overshadows ballistic or quasi-ballistic light.

For breast tissue of clinically useful thickness (5 to 10 cm), scattered light must be used to image breast cancers. We have shown that for a 5-cm-thick breast tissue with the assumed absorption coefficient $\mu_a = 0.1\ cm^{-1}$, reduced scattering coefficient $\mu_s' = 10\ cm^{-1}$, the detector must collect transmitted light that has experienced at least 1100 scattering events in tissue to yield enough signal.[4] Therefore, ballistic light or even quasi-ballistic light does not exist for practical purposes. However, if a 10-mW visible or near IR laser is incident on one side of the 5-cm thick breast tissue, we have estimated using diffusion theory that the diffuse transmittance on the other side is on the order of 10 nW/cm^2 or 10^{10} photons/(s•cm^2), which is detectable using a photomultiplier tube capable of single-photon counting. Similarly, the diffuse transmittance through a 10-cm thick breast tissue would be on the order of 1 pW/cm^2 or 10^6 photons/(s•cm^2).

To utilize the diffuse light for its abundance and overcome its lack of direct imaging information, ultrasound-modulated optical tomography of turbid media has been studied. Marks et al have investigated tissue imaging using the combination of pulsed ultrasound and laser light and have detected the ultrasound-modulated optical signal in a homogeneous turbid medium without buried objects.[5] Wang et al developed ultrasound-modulated optical tomography that combined continuous-wave ultrasound and laser irradiation and successfully imaged buried objects in tissue-simulating turbid media.[1,2] The major advantage of using continuous-wave ultrasonic modulation over pulsed ultrasonic modulation is the significant increase in signal-to-noise ratio. Leutz and Maret reported the observation of ultrasonic modulation of multiple light scattering speckles.[6] Kempe et al investigated the modulation of the optical field transmitted through a turbid medium by a quasi-continuous-wave ultrasound beam.[7]

We report in this paper the theoretical considerations and experimental results of our recent studies. Modulated signal was calculated using diffusion theory. The dependence of the ultrasound-modulated optical signal on the off-axis distance of the detector from the optic axis was studied. The mechanisms of ultrasonic modulation of light were discussed.

Hypothesis

The design of the experiment on ultrasound-modulated optical tomography was based on the following hypothesis (**Fig. 1**). Continuous-wave ultrasound wave was propagated through a turbid medium and focused to a small spot inside the medium. The ultrasound wave modulated light passing through the ultrasonic field.

Several possible modulation mechanisms are discussed as follows (**Fig. 2**). Ultrasound wave generated pressure variation (approach 1). The pressure variation induced a density change in the medium as a result of the compressibility of the medium. The optical absorption and scattering coefficients were proportional to the number density of absorbers and scatterers, respectively. The index of refraction varied with the density as well. Therefore, the density variation modulated the optical properties of the medium at the ultrasound frequency. The variation of optical properties modulated the light passing through the ultrasonic field.

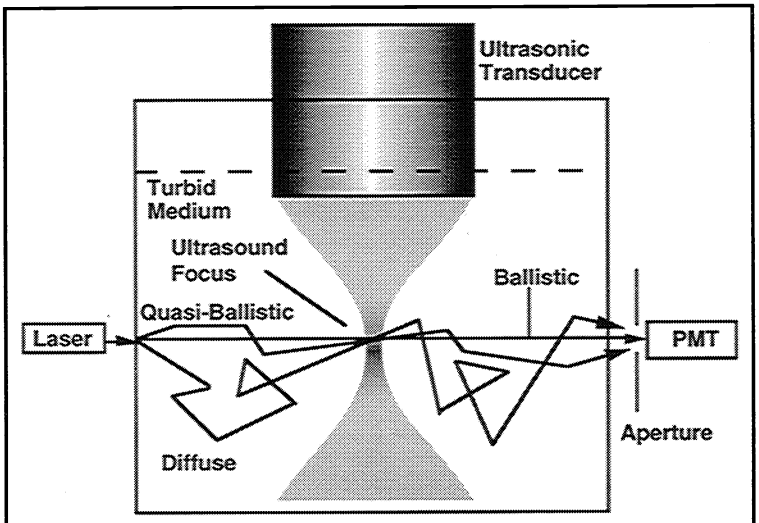

Fig. 1. Illustration of the *hypothesis* of ultrasound-modulated optical tomography. The ultrasound-modulated light carries the information of the optical and mechanical properties at the ultrasonic focal spot, which provides a localization mechanism for optical imaging.

Ultrasound wave generated particle displacement (approach 2). The particle displacement caused optical pathlength to change. Coherent laser light passing through turbid media generated speckles. Because speckles depended on the optical pathlength, the speckles varied at the ultrasonic frequency.

Ultrasound wave may be considered as phonons, whereas light may be considered as photons (approach 3). The photon-phonon interaction caused Doppler shift[8] of the optical frequency by the ultrasonic frequency. An optical detector functioned as a heterodyning device between the Doppler-shifted light and unshifted light and produced a signal of the ultrasonic frequency.

The modulated light carried the information of the optical and mechanical properties near the focal spot, where the modulation off focus was assumed less than that at the focus. The ultrasound-modulated light signal can be separated from the unmodulated light signal by an electronic filter. Scanning the imaging system relative to the turbid medium would generate an image of the medium based on the distribution of optical and mechanical properties. The ultrasonic modulation depended on any light, which was primarily *diffuse light* rather than ballistic or quasi-ballistic light for dense turbid medium. The imaging resolution depended on the size of the ultrasonic focus.

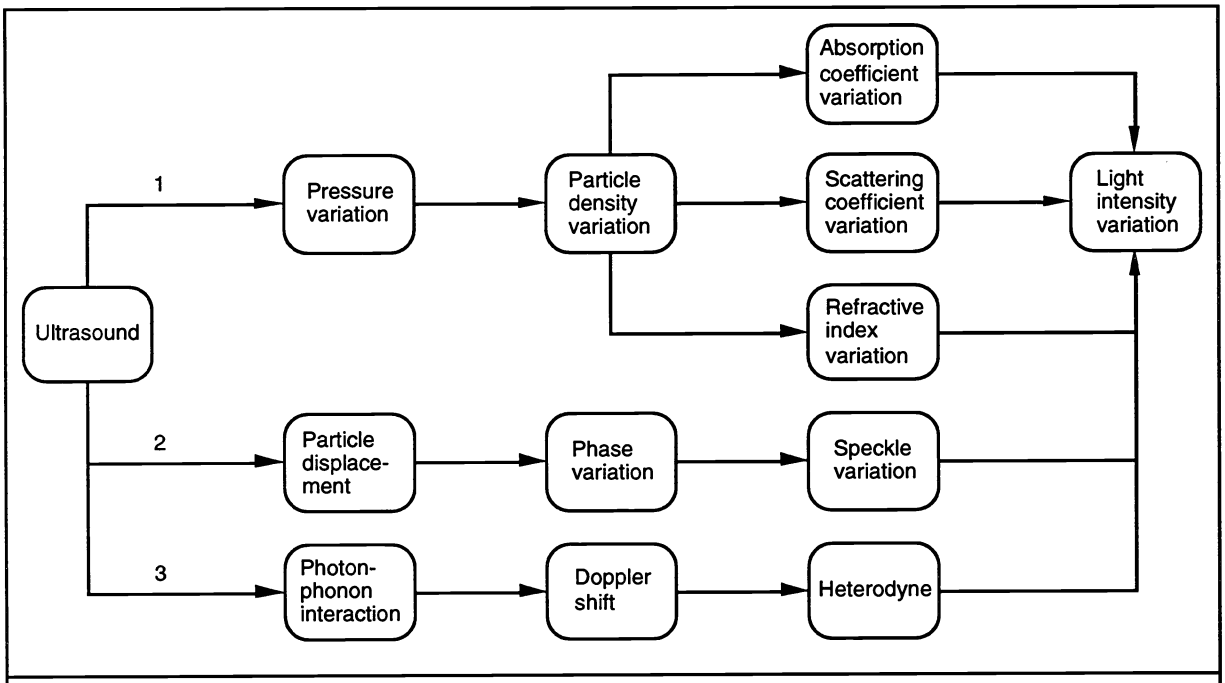

Fig. 2. List of possible mechanisms of ultrasonic modulation of light in turbid media.

Theoretical Considerations

Detectability of ultrasonic modulation of diffuse light was estimated using diffusion theory for an infinite turbid medium. The following Green's function was used to estimate photon transport from an isotropic point source to a point of observation in the medium.

$$G(r) = P_s \exp(-\mu_{eff} r) / (4 \pi D r) \quad (1)$$

where

G(r): fluence rate at the point of observation that was r away from the light source [W/cm^2].

r: distance between the point of observation and the light source [cm].

P_s: power of the light source [W].

μ_{eff}: effective attenuation coefficient [cm^{-1}].

D: diffusion constant [cm].

The effective attenuation coefficient and the diffusion constant were calculated based on the optical properties of the turbid medium.

$$D = 1/[3 (\mu_a + \mu_s')] \quad (2)$$

$$\mu_{eff} = \sqrt{\mu_a/D} \quad (3)$$

where

μ_a: absorption coefficient of the turbid medium [cm^{-1}].

μ_s': reduced scattering coefficient of the turbid medium [cm^{-1}].

A collimated laser beam may be modeled using an isotropic point source that was 3D away from the incidence point along the direction of the laser beam. For the optical properties and geometry we considered, the distance 3D was insignificant compared with the distance between the light source and the point of observation. Therefore, the collimated laser beam was replaced with an isotropic point source for simplicity without losing the validity of estimation.

Some of the light from the source was transported to the ultrasonic focus, modulated by the ultrasound, then transported to the detector. The detected signal may be estimated using the Green's function given by Eq. (1). The modulated signal at the focus was considered a source and re-emitted.

$$\phi_{ac} = G(r_{sf})\, A_m\, m\, G(r_{fd}) \tag{4}$$

where

ϕ_{ac}: fluence rate at the detector [W/cm^2].

r_{sf}: distance between the light source and the ultrasonic focus [cm].

A_m: surface area of ultrasound-modulation volume [cm^2].

m: modulation depth of light intensity [–].

r_{fd}: distance between the ultrasonic focus and the detector [cm].

The flux into the detector may be calculated from the fluence rate at the detector as follows.

$$J_+ = \frac{\phi_{ac}}{4} - \frac{D}{2}\left.\frac{\partial \phi_{ac}}{\partial z}\right|_{z = r_{fd}} = \frac{\phi_{ac}}{4}\left[1 + 2\,D\,(\mu_{eff}\, r_{fd} + 1)/r_{fd}\right] \tag{5}$$

where

J_+: flux (current density) into the detector in the +z direction [W/cm^2].

z: axis from the light source to the detector [cm].

The detected power can be calculated by

$$P_d = J_+\, A_d \tag{6}$$

where

P_d: detected power [W].

A_d: detection area of the detector [cm^2].

Table I lists the calculated results for various parameters. The surface area of modulation was assumed to be that of a cylinder of 0.2 cm in diameter and 0.2 cm in height. The modulation depth m was assumed to be 10^{-5}. The source power P_s of the laser was assumed to be 0.01 W. The detection area of the detector was assumed to be 1 cm^2.

Table I. Results of theoretical calculation.

μ_a [cm^{-1}]	μ_s' [cm^{-1}]	r_{sf} [cm]	r_{fd} [cm]	P_d [W]	N_d [1μm photons/sec]
0.02	10	2.5	2.5	9.6×10^{-11}	4.8×10^{8}
0.02	10	0.5	4.5	2.6×10^{-10}	1.3×10^{9}
0.02	10	5	5	4.9×10^{-13}	2.5×10^{8}
0.1	10	2.5	2.5	8.3×10^{-13}	4.2×10^{6}
0.1	10	0.5	4.5	2.3×10^{-12}	1.2×10^{7}
0.1	10	5	5	3.4×10^{-17}	1.7×10^{2}

The units W for the detected power P_d may be converted into photons/sec based on the photon energy. For 0.5 μm wavelength light, 1 J energy contains 2.5×10^{18} photons. For 1 μm wavelength light, 1 J energy contains 5.0×10^{18} photons. If 1 μm wavelength is used, 9.6×10^{-11} W corresponds to 4.8×10^{8} photons/sec, and 3.4×10^{-17} W corresponds to 170 photons/sec.

Experimental Methods

Liquid tissue phantoms (turbid media) were prepared to simulate the optical properties of tissues by dissolving dominantly absorbing Trypan blue dye and dominantly scattering Intralipid in water. Similarly, gel tissue phantoms were prepared by dissolving Trypan blue dye and Intralipid in 5% (by weight) gelatin solutions. The optical properties were controlled by varying the amount of absorbers and scatterers. The phantom was contained in a 5-cm thick cuvette. An ultrasonic absorber was placed at the bottom of the cuvette to avoid ultrasonic reflection. Two other ultrasonic absorbers were placed inside the two sides of the cuvette.

The compressibility of water is 4.6×10^{-5} bar^{-1}. The compressibility of breast fat is approximately 5.4×10^{-5} bar^{-1}.[9] The compressibility of the gel phantom should be on the same order of that of water because we did not observe significant change in ultrasound-modulated optical signal between the water phantom and gel phantom when both phantoms had the same absorption and reduced scattering coefficients.

To make a gel phantom containing a buried object, the gel phantom was placed inside the cuvette before it coagulated in a refrigerator. Another small gel phantom cube was placed inside the background gel in the mid-plane. The facets of the cube were parallel with those of the cuvette. A liquid phantom that had identical optical properties as the background gel was poured into the cuvette to couple ultrasonic wave and allow the scanning of ultrasonic transducers.

A block diagram of the experimental setup is shown in **Fig. 3**. The glass cuvette containing turbid medium was seated on a two-dimensional translation stage. While the cuvette was translated, the rest of the system, including the optical and ultrasonic systems, were fixed.

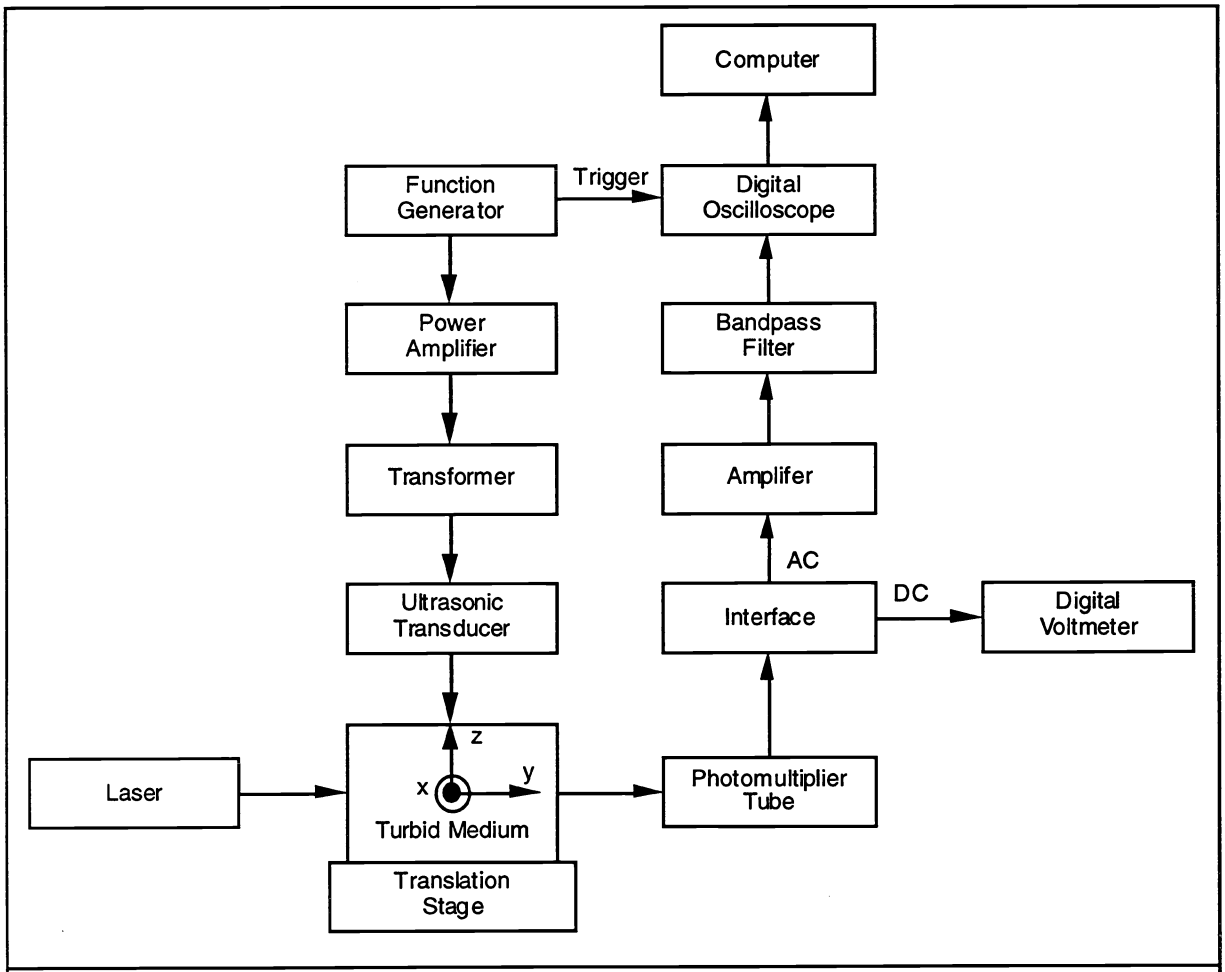

Fig. 3. A block diagram of the experimental setup.

A He-Ne laser with 10-mW output power and 632.8-nm wavelength delivered a single-mode Gaussian beam perpendicular to the front surface of the cuvette. The lower end of the ultrasonic transducer was buried in the liquid phantom to allow a good coupling of the ultrasound wave. The room lights were turned off to reduce the ambient noise collected by the photomultiplier tube (PMT). An aperture was placed in front of the PMT to control the amount of light entering the PMT.

A function generator produced a sinusoidal wave at a fixed frequency of 1 MHz. This signal drove the ultrasonic transducer after being amplified to 45 V amplitude by a power amplifier and a transformer.

The operating bandwidth of the ultrasonic transducer was centered at 1 MHz. The diameter of the active element of the ultrasonic transducer was 1.9 cm. The focal length of the transducer in water was 3.68 cm. The diameter of the ultrasonic focal spot in water was 0.29 cm. The consumed electric power by the transducer was 210 mW, ~50% of which was converted into acoustic power. The peak pressure at the focus was ~2 bars, which was below the maximum allowed pressure for ultrasonic diagnostics. One can convert the acoustic peak pressure into average intensity and further into power deposition if those quantities are of interest. The peak pressure is of immediate interest for ultrasonic modulation of optical properties and particle displacement.

After light passed through the aperture and reached the PMT, the optical signal was converted into electrical signal. The electrical signal was separated into DC and AC components by an interface circuit. The DC voltage was read by a digital voltmeter, and the AC voltage was amplified and then effectively filtered by a narrow bandpass filter. The filtered signal was collected and averaged over 500-1000 sweeps by the digital oscilloscope, which was triggered by a reference signal from the function generator. Both the frequency filtering and signal averaging enhanced the signal-to-noise ratio. The averaged time-domain signal was then transferred to a computer for data storage and processing. The peak-to-peak voltage of the AC signal represented the ultrasound-modulated optical signal, whereas the DC signal represented the unmodulated optical signal.

To study the dependence of the AC signal on the off-axis position of the PMT from the optic axis, we translated the detector gradually away from the center and recorded the AC signal at each detector position. To obtain an image of the turbid medium, the cuvette was translated and the AC signal was recorded at each position. Once the signals of all the scanned positions were obtained, an image of the turbid medium containing a buried object was constructed.

For convenience, we set up a Cartesian coordinate system to represent the position of the turbid medium. The x-axis was a horizontal axis perpendicular to the optic axis. The y-axis was the optic axis defined by the laser beam. The z-axis was the ultrasonic axis that was defined by the ultrasonic wave.

Results

The peak-to-peak AC voltage was recorded for various PMT positions along the horizontal x-axis (**Fig. 4**). The optical properties of the 5-cm thick homogeneous liquid turbid medium were absorption coefficient $\mu_a = 0.1\ cm^{-1}$ and reduced scattering coefficient $\mu_s' = 6.2\ cm^{-1}$. The aperture in front of the PMT was 2.1 cm diameter. The PMT was first centered on the optic axis (y-axis)

and was then translated away from the optic axis with a 1-mm step size. The AC voltage was obtained at each PMT position by measuring its peak-to-peak voltage on the oscilloscope.

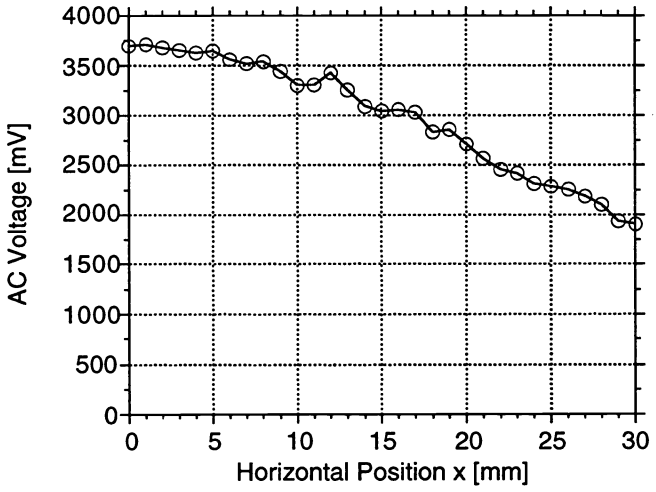

Fig. 4. The peak-to-peak AC voltage as a function of the horizontal position of the PMT on the x-axis.

A 2D image of a clear object buried inside a turbid medium was obtained by raster scanning the turbid medium (**Fig. 5**). Both the buried object and the background medium were made of gels. The buried object was approximately a 6-mm wide cube. The optical properties of the 5-cm thick background turbid medium were absorption coefficient μ_a = 0.1 cm^{-1} and reduced scattering coefficient μ_s' = 10 cm^{-1}. The optical properties of the buried object contained no absorbers or scatterers. The turbid medium was translated along the x- and z-axes with a 1-mm step size. The ultrasound-modulated optical signal (AC signal) was recorded at each position. A 2D density plot was then generated.

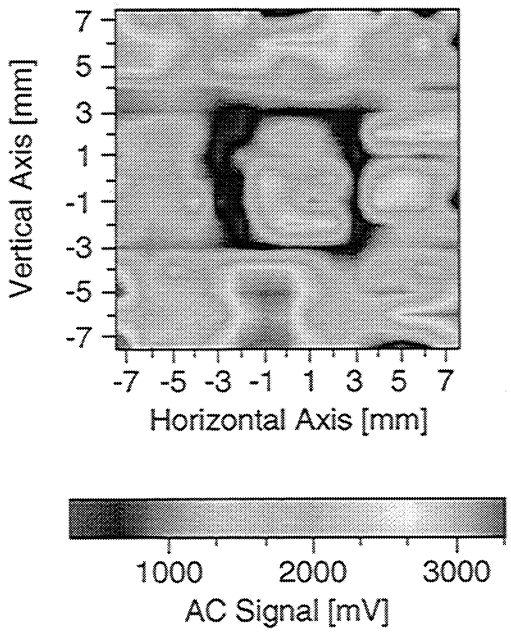

Fig. 5. 2D image of a clear object buried in a turbid medium using ultrasound-modulated optical tomography.

Conclusions and Discussion

The signal of ultrasonic modulation of transmitted light was carefully tested to rule out the possibility of interference. When the ultrasonic wave was turned off or blocked using an ultrasound-absorbing rubber, the AC signal was reduced to the noise level, which was the shot noise caused by the transmitted unmodulated light. When the laser light was blocked and the ultrasonic wave was kept on, the AC signal was reduced to nearly zero on the oscilloscope, which was essentially a measurement of the dark current in the PMT and the ambient light in the dark room. Therefore, the AC signal must have been generated by the interactions between the ultrasonic wave and the laser light.

The DC signal was measured ~50 V while the AC amplitude was ~700 mV. Based on the gains of the AC and DC branches, the ratio between the AC and DC currents at the PMT anode was estimated to be on the order of 10^{-5}-10^{-6}. The modulation was weak because the compressibility of the medium was on the order of 4.6×10^{-5} bar^{-1} and the peak pressure at the ultrasonic focus was 2 bars. Furthermore, some transmitted light bypassed the ultrasonic field. The incoherent addition of multiple coherence areas on the detector maybe another factor causing the low modulation depth.[7]

A related question was about the acoustic power deposition in the medium. For the peak acoustic pressure at focus $p_0 = 2$ bars, the average acoustic intensity (power density) was

$$I = p_0^2 / (2 \rho c) = (2\times10^5 \text{ Pa})^2 / [2 \times 1.5\times10^6 \text{ kg/(s m}^2)] = 1.3 \text{ W/cm}^2$$

where ρc was the acoustic impedance of the medium. The acoustic absorption in soft tissue μ_a was ~3×10^{-2} cm^{-1}.[9] The peak power deposition was

$$Q = \mu_a I = 3 \times 10^{-2} \times 1.3 \text{ W/cm}^3 = 0.039 \text{ W/cm}^3$$

The thermal relaxation time at the 0.29 cm diameter focus was

$$\tau = r^2 / \kappa = (0.145 \text{ cm})^2 / 1.3 \times 10^{-3} \text{ cm}^2\text{/s} = 16 \text{ s}$$

where r was the radius of the focal zone, and κ was the thermal conductivity. The temperature rise during the thermal relaxation time was

$$\Delta T = Q \tau / C = 16 \times 0.039/3.1 = 0.2 \text{ °K},$$

assuming there was no heat conduction during the thermal relaxation time. The specific heat of soft tissue C is 3.1-3.9 J/(g•K). This estimated temperature rise would be reduced when (1) the peak power position was spatially averaged , (2) the thermal diffusion and blood perfusion was considered, or (3) the sampling time was shorter than the thermal relaxation time (16 s). A temperature rise threshold of 2 °C would be allowed by ultrasound safety standards.[10]

Fig. 4 demonstrated that the ultrasound-modulated optical signal depended on diffuse light rather than ballistic light. If the ultrasound-modulated optical signal depended on ballistic light, the signal would disappear when the PMT was moved away from the optic axis. The gradual decrease

of the AC signal indicated that the ultrasound-modulated optical signal originated from the interactions between diffuse light and ultrasound.

The mechanisms of ultrasonic modulation of light may be classified into three approaches as shown in Fig. 2: (1) intensity modulation, (2) phase modulation, and (3) frequency shift. The intensity modulation does not require coherence of the light source. The phase modulation is a coherent speckle effect.[6,7] The frequency shift is caused by photon-phonon interactions and requires coherence as well.

The frequency shift approach may be merged into the phase modulation approach if the ultrasonic modulation of index of refraction was taken into account in the calculation of the optical path length. However, we considered the two approaches separately for clarity, where the path length did not include the effect of the ultrasonic modulation of index of refraction.

A key question was which approach was dominant in our experiments. Incoherent wide-band flash light was used to replace the laser light to examine the intensity modulation approach. No ultrasound-modulated optical signal was observed experimentally. This preliminary experiment disfavored the intensity modulation approach because the intensity modulation approach should not require coherence of the light source.

The buried clear object was imaged to test the dependence of the signal on scatterers (Fig. 5). The signal from the buried object was comparable with that outside the object. This result indicated that a path length variation induced by the ultrasonic vibration of scatterers was not necessary to produce ultrasound modulation of light. At first glance, we tended to think that approach 3 (photon-phonon interactions) was the dominant mechanism and approach 2 could be ruled out. The signal from the clear object should have been based on approach 3 because the clear object was free of scatterers. However, the contribution of approach 2 was still unclear when the ultrasonic focus was in turbid medium. Therefore, further studies are needed to evaluate the relative importance of approaches 2 and 3 under various conditions. The dark boundary in Fig. 5 was possibly caused by the imperfect preparation of burying object, which had produced an unwanted acoustic boundary.

The theoretical calculation predicted a modulated signal of approximately 8.3×10^{-13} W at the detector for $\mu_a = 0.1$ cm^{-1}, $\mu_s' = 10$ cm^{-1}, and 5 cm thickness. The observed AC voltage under these conditions was ~700 mV. Based on the gains of the PMT and the AC amplifier in the experimental setup, the estimated AC power was on the order of 10^{-13} W. This agreement could have been fortuitous because the theory did not take heterodyne into account. Nevertheless, the raw modulated signal was not very strong and competing with the shot noise. A sensitive detection system was essential to acquire a good S/N.

Summary

It was experimentally proved that ultrasound-modulated optical signal depended on diffuse light rather than ballistic light. Coherent approaches were likely the dominant mechanism of ultrasonic modulation of light in our experiments on dense turbid media.

Acknowledgment

This project was sponsored in part by the National Institutes of Health grant R29 CA68562 and The Whitaker Foundation.

References

1. L.-H. Wang, S. L. Jacques, and X.-M. Zhao, "Continuous-wave ultrasonic modulation of scattered laser light to image objects in turbid media," Optics Letters **20**, 629-631 (1995).
2. L.-H. Wang, X.-M. Zhao, and S. L. Jacques, "Ultrasound-modulated optical tomography for dense turbid media," Proc. Soc. Photo-Opt. Instrum. Eng. **2676**, 91-102 (1996).
3. R. R. Alfano (ed.), Proc. of Advances in Optical Imaging and Photon Migration, in press (1996), Optical Society of America.
4. L.-H. Wang and S. L. Jacques, "Application of probability of n scatterings of light passing through an idealized tissue slab in breast imaging," Proc. of Advances in Optical Imaging and Photon Migration **21**, 181-186 (1994).
5. F. A. Marks, H. W. Tomlinson, and G. W. Brooksby, "A comprehensive approach to breast cancer detection using light: photon localization by ultrasound modulation and tissue characterization by spectral discrimination," Proc. Soc. Photo-Opt. Instrum. Eng. **1888**, 500-510 (1993).
6. W. Leutz and G. Maret, "Ultrasonic modulation of multiply scattered light," Physica B **204**, 14-19 (1995).
7. M. Kempe, M. Larionov, D. Zaslavsky, and A. Z. Genack, "Acousto-optic tomography with multiply-scattered light," Proc. of Advances in Optical Imaging and Photon Migration, in press (1996).
8. A. Korpel, *Acousto-Optics* (Marcel Dekker, Inc., New York, 1988).
9. F. A. Duck, *Physical Properties of Tissue: a Comprehensive Reference Book* (Academic Press, London, New York, 1990).
10. T. A. Whittingham, "The safety of ultrasound," Imaging **6**, 33-51 (1994).